processes

MDPI

Article

Rheological Properties of Film-Forming Gels Based on Collagen from *Octopus maya* By-Products and Food-Grade Polysaccharides

María Fernanda Acosta-Pacheco [1], Élida Gastélum-Martínez [1], Juan Valerio Cauich-Rodríguez [2], Ingrid Mayanin Rodríguez-Buenfil [1] and Manuel Octavio Ramírez-Sucre [1,*]

[1] Sede Sureste, Centro de Investigación y Asistencia en Tecnología y Diseño del Estado de Jalisco A.C., Tablaje Catastral 31264, Km 5.5 Carretera Sierra Papacal-Chuburná Puerto, Parque Científico y Tecnológico de Yucatán, Mérida C.P. 97302, Yucatán, Mexico; feacosta_al@ciatej.edu.mx (M.F.A.-P.); egastelum@ciatej.mx (É.G.-M.); irodriguez@ciatej.mx (I.M.R.-B.)

[2] Unidad de Materiales, Centro de Investigación Científica de Yucatán, Calle 43 No. 130 x 32 y 34, Colonia Chuburná de Hidalgo, Mérida C.P. 97205, Yucatán, Mexico; jvcr@cicy.mx

* Correspondence: oramirez@ciatej.mx

Abstract

Octopus maya is a fast-growing species from the Yucatán Peninsula with high economic relevance, accounting for a major share of regional fishery production. However, a significant fraction of the organism, rich in type I collagen, is discarded as by-products, representing a promising and underutilized source for sustainable biomaterials. This study evaluated, through a 3^2 factorial design, the effect of two factors on the rheological and dynamic mechanical properties of film-forming solutions (FFS). The first factor was the type of food-grade polysaccharide: chitosan (Ch), hydroxypropyl methylcellulose (HPMC), or starch (S). The second factor was the proportion of each polysaccharide blended with ultrasound-extracted *Octopus maya* insoluble collagen (CIPM), using polysaccharide ratios of 30:70, 50:50, and 70:30 (*w*/*w*). This approach aims to valorize octopus by-products through the recovery and functional utilization of collagen. Rheological properties were determined by rotational and oscillatory rheometry at 25 °C, with flow curves fitted to the Carreau-Yasuda model. All formulations exhibited pseudoplastic behavior ($n < 1$), with viscosity decreasing as shear rate increased. Pure CIPM showed high viscosity (190.36 Pa·s at 1 s^{-1}), which decreased (0.3–10.44 Pa·s) in HPMC and chitosan systems, suggesting their potential suitability for applications requiring fluidity, such as spray coatings or film-forming solutions, based on their rheological properties. In contrast, starch-based systems exhibited higher viscosities (33.54–197.53 Pa·s) and a more structured viscoelastic profile ($G' > G''$), suggesting potential suitability for thick coatings or gels requiring structural stability, although these applications were not experimentally validated. These results demonstrate that CIPM-polysaccharide systems enable tunable rheological properties, supporting the use of *Octopus maya* collagen as a sustainable functional material for advanced food and biomaterial design.

Keywords: *Octopus maya* by-products; insoluble collagen; ultrasound-assisted extraction; rheological characterization; film-forming solutions

Check for updates

Academic Editor: Pavel Mokrejš

Received: 2 June 2026
Revised: 28 June 2026
Accepted: 29 June 2026
Published: 6 July 2026

Copyright: © 2026 by the authors. Licensee MDPI, Basel, Switzerland. This article is an open access article distributed under the terms and conditions of the Creative Commons Attribution (CC BY) license.

1. Introduction

Film-forming solutions (FFS) are biopolymeric systems composed of proteins and/or polysaccharides capable of producing biodegradable films for food applications [1]. In-

teractions among these biopolymers can alter the viscosity, texture, and stability of the system through the formation of three-dimensional viscoelastic networks [2,3]. In these networks, polysaccharides (PS) directly influence the formation of viscoelastic gels that serve as the structural basis of the films, modifying the viscosity, microstructure, and barrier properties of the material due to their gelling ability and biodegradability. Three polysaccharides commonly used in food systems were selected for this study: (1) hydroxypropyl methylcellulose (HPMC, H), because of its ability to form thermoreversible gels between 50 and 90 °C and to produce transparent and resistant films, with tensile strength values close to 11 N and puncture resistance of approximately 6 N in 3% solutions [4,5]; (2) chitosan (Ch), due to its biodegradability, antimicrobial properties, and ability to improve the mechanical performance of biodegradable films, increasing tensile strength from 2.3 to 6.3 MPa and elongation from 50 to 63% [6,7]; and (3) corn starch (S), because of its abundance, renewability, and biodegradability, as well as its thickening capacity associated with amylopectin content (73%) and its structuring and gelling properties attributed to amylose (27%) [8].

In this context, collagen is a structural protein widely distributed in animal tissues. Approximately 28 collagen types have been identified, with type I collagen being the most abundant in connective tissues [9]. It is characterized by its gelling ability and capacity to form viscoelastic matrices with predominantly elastic behavior ($G' > G''$), while also providing texturizing and stabilizing properties to the system [10]. Although the main commercial sources of collagen type I are bovine and poultry by-products, in which collagen accounts for nearly 30% of the total protein content [11], highly purified type I collagen remains relatively expensive. Depending on its purity grade and intended application, commercial prices may range from approximately 4.5 to 7.0 USD/g for reagent-grade products commonly used in laboratories and biomaterial applications. In this sense, marine sources such as fish, squid, jellyfish, and *Octopus maya* have attracted increasing interest due to their higher sanitary safety and high extraction yields, which may exceed 80% depending on the species and extraction method employed [12]. In cephalopods such as squid and octopus, rapid metabolism influences the composition and structure of connective tissue, thereby affecting collagen solubility. In addition, the absence of ethical or religious restrictions positions marine sources as a viable alternative to terrestrial sources [12,13].

Octopus maya is a fast-growing species distributed throughout the Yucatán Peninsula and represents a highly important fishery resource. According to the Comisión Nacional de Acuacultura y Pesca [14], octopus accounts for 66% of fishery production in Yucatán, with approximately 40,000 tons captured annually, generating an estimated economic value of nearly 2000 million Mexican pesos (approximately 115 million USD) through its commercialization and consumption. However, only 74% of the organism, mainly the arms, is commercially utilized, whereas the remaining 26%, corresponding to the mantle, tips, and viscera, is considered a by-product [15]. These by-products constitute a viable source of predominantly type I collagen, as collagen contents of up to 38% have been reported in cephalopod connective tissue [15–17]. These facts support their potential application in fishery waste valorization and the development of sustainable functional materials.

The rheological properties of FFS are closely linked to the performance of the resulting films and depend on factors such as component compatibility, polymer and plasticizer ratios, and the order of ingredient addition. Previous studies have reported protein-to-polysaccharide ratios ranging from 20:80 to 80:20 and plasticizer contents between 0.5 and 1.5% [18–20]. These formulations enable the production of uniform, flexible, and thin films, generally with thicknesses below 0.3 mm [21], making them suitable for food and packaging applications [22,23].

Although the effects of polysaccharides in film-forming systems have been widely documented, their behavior in combination with insoluble collagen obtained from *Octopus maya* by-products remains unexplored. This limits the functional utilization of these by-products in applications such as edible coatings and biodegradable packaging. Insoluble collagen from *Octopus maya* (CIPM) represents a promising fraction due to its hydrated gel-like behavior and its suitability for incorporation into film-forming solutions. The selection of CIPM was based on these rheological properties, which motivated its evaluation in combination with food-grade polysaccharides. Therefore, this study evaluated the effect of polysaccharide type and proportion (HPMC, Ch, and S) in mixtures with insoluble collagen from *Octopus maya* (CIPM) on the rheological properties of FFS, including viscosity, storage modulus (G'), loss modulus (G''), and tan δ. This study contributes to the evaluation of these formulations for the development of functional materials for the food industry while promoting the sustainable valorization of marine by-products.

2. Materials and Methods

2.1. Extraction of Collagen from Octopus maya

Insoluble collagen from *Octopus maya* (CIPM) was obtained from raw by-products (mantle and arm tips) collected from specimens captured during the 2023–2024 fishing season along the coast of Yucatán, Mexico, in accordance with the guidelines established in NOM-008-PESC-1993. The organisms were provided through the project "Plataforma tecnológica pulpo maya para el desarrollo de productos de alto valor agregado 6559" and subsequently stored frozen until processing, following the procedure described by Ocampo-García [15].

The by-products were homogenized and subjected to an alkaline pretreatment with 0.1 M NaOH (pellets, analytical grade, Vetec, Duque de Caxias, RJ, Brazil, 700 mL per 100 g of sample) using an ultrasonic bath (Bransonic® 3510R-MT, Branson Ultrasonics Corporation, Danbury, CT, USA) for 15 min while maintaining the temperature below 35 °C. The alkaline supernatant was removed by centrifugation (4 °C, 20 min, 4500 rpm), and the solid fraction was washed with distilled water until residual NaOH was eliminated, yielding the pretreated material for acid extraction. The pretreated material was subsequently treated with glucono-δ-lactone (700 mL, GDL, ≥99.0%, G4750, Sigma-Aldrich, St. Louis, MO, USA) under ultrasonic conditions for 3 h while maintaining the temperature below 35 °C. After a second centrifugation step (4 °C, 20 min, 4500 rpm), two fractions were obtained: the supernatant (soluble fraction) and a gel-like precipitate (insoluble fraction). The insoluble fraction (5.31% of the recovered mass) was selected for this study because of its hydrated gel-like behavior. SDS-PAGE analysis revealed α1 chains between 90 and 100 kDa and α2 chains between 85 and 90 kDa, together with bands above 100 kDa corresponding to β components, a banding pattern consistent with type I collagen. In addition, the total amino acid composition, expressed as mg/100 g, confirmed the presence of amino acids commonly found in collagen, including glycine, proline, and alanine. Together, these analyses supported the identification of the insoluble fraction as a collagen-rich fraction (Supplementary Materials: Figure S1–Table S1). Finally, a commercial protocol for lyophilized bovine type I collagen supplied by Advanced BioMatrix (catalog. 5162) was adapted with minor modifications. Specifically, 0.04 M HCl (HCl, Sigma-Aldrich, St. Louis, MO, USA) was used for gel homogenization due to the gel-like nature of the extracted collagen.

2.2. Preparation of Film-Forming Solutions (FFS)

Analytical-grade polysaccharides used in this study included corn starch (S4126), high-molecular-weight chitosan with ≥75% degree of deacetylation (DA) (419419), and

hydroxypropyl methylcellulose (HPMC) (423238), all purchased from Sigma-Aldrich (St. Louis, MO, USA). These polysaccharides were dissolved at different concentrations (Table 1) together with BioXtra glycerol ≥ 99.0% (GC) (G6279, Sigma-Aldrich, St. Louis, MO, USA) as a plasticizing agent, using proportions that allowed the formation of film-forming solutions with adequate structural integrity after drying by the casting method [19]. For film preparation, 16 mL of solution was poured into polystyrene Petri dishes and dried for 24 h at 45 ± 2 °C in a Heratherm® OGH100 oven (Thermo Scientific, Waltham, MA, USA). HPMC and corn starch were solubilized in distilled water at 60 °C and 90 °C, respectively, according to the supplier's technical recommendations. Chitosan was dissolved in 1% acetic acid (Sigma-Aldrich, St. Louis, MO, USA), and an ultrasonic bath (Ultrasonic Cleaner Bransonic™ B200, Branson Ultrasonics Corporation, Danbury, CT, USA) for 3 min (220 V, 50/60 Hz) was used to remove bubbles. CIPM was dispersed in 0.04 M HCl for 1.5 h until a homogeneous mixture was obtained. Once all systems were solubilized, glycerol was incorporated according to the proportions shown in Table 1.

Table 1. Composition of film-forming solutions.

Nomenclature	Base of FFS System	Concentration (%)	
		Polysaccharide	Glycerol
FFS-CIPM	Insoluble collagen	3	0.6
FFS-H	HPMC	2	1
FFS-Ch	Chitosan	0.5	0.6
FFS-S	Starch	2.5	2

CIPM: Insoluble collagen from *Octopus maya*; HPMC: Hydroxypropyl methylcellulose.

The film-forming solution based on insoluble collagen from *Octopus maya* (FFS-CIPM) was mixed for 2 min until complete homogenization with the different polysaccharide-based film-forming solutions (FFS-PS): (1) FFS-H (HPMC), (2) FFS-S (starch), and (3) FFS-Ch (chitosan). The mixtures were prepared at the selected weight ratios of 30:70, 50:50, and 70:30 (FFS-CIPM:FFS-PS).

2.3. Rheological Characterization

2.3.1. Flow Behavior

Flow behavior and viscoelastic properties of the FFS were evaluated according to the methodology described by Ramirez-Sucre and Baigts-Allende [24], with minor modifications. Briefly, measurements were performed using a controlled-stress hybrid rheometer (Discovery DHR-2 Hybrid Rheometer, TA Instruments, New Castle, DE, USA) equipped with a Peltier temperature-controlled plate system and a 40 mm parallel plate geometry (Peltier Sandblasted—104770, TA Instruments, New Castle, DE, USA) with a gap of 1050 µm. Approximately 2 mL of each sample was loaded at 25 °C and allowed to equilibrate for 5 min prior to analysis.

Viscosity curves were obtained as a function of shear rate over a range of 0.001 to 100 s^{-1}. The experimental data were fitted to the Carreau-Yasuda model (Equation (1)) using TRIOS software v5.7.2.101. This model was selected because it provided the best fit for flow parameters and high predictive accuracy for pseudoplastic biopolymeric systems, with a coefficient of determination of R^2 = 0.999.

Equation (1). Carreau-Yasuda model

$$\frac{\eta - \eta_\infty}{\eta_0 - \eta_\infty} = \left[1 + (k\dot{\gamma}^{\alpha})\right]^{\frac{n-1}{\alpha}} \quad (1)$$

where η is the viscosity, η_0 is the zero-shear viscosity, η_∞ is the infinite-shear viscosity, k is the consistency index, $\dot{\gamma}$ is the shear rate, n is the flow behavior index, and α is the transition parameter.

2.3.2. Viscoelastic Behavior

To evaluate the viscoelastic response, oscillatory strain sweep tests were performed over a deformation range of 0.01–100% at a constant frequency of 1 Hz to determine the linear viscoelastic region (LVR). Frequency sweep tests were subsequently conducted from 0.01 to 100 Hz using a deformation value (0.1%) within the LVR. Storage modulus (G′), loss modulus (G″), and tan δ values were obtained as a function of frequency (Hz) from the dynamic mechanical spectra.

2.4. Experimental Design and Statistical Analysis

A 3^2 factorial design was implemented to evaluate the effect of two factors: (1) polysaccharide type (HPMC, starch, or chitosan) and (2) FFS-CIPM:FFS-PS ratio (30:70, 50:50, and 70:30, *w*/*w*) on the rheological and dynamic mechanical properties of the systems. The response variables for flow behavior included apparent viscosity (Pa·s) measured at 1 s^{-1} and the Carreau-Yasuda model parameters (η_0, η_∞, k, n, and α). For dynamic mechanical behavior, the response variables included the viscoelastic parameters storage modulus (G′), loss modulus (G″), and tan δ at 1 Hz. All formulations were independently prepared in duplicate, and rheological measurements were performed on each preparation. Results are reported as mean ± standard deviation (n = 2).

Statistical analysis was performed using Statgraphics Centurion XVI software (v.16.1.03). Data were analyzed by analysis of variance (ANOVA) at a 95% confidence level ($p < 0.05$) to determine the effects of the studied factors and their interactions on the response variables.

3. Results and Discussion

3.1. Flow Behavior of Systems

3.1.1. Flow Behavior of Control Film-Forming Solutions

Control film-forming solutions (FFS) prepared with each polysaccharide and glycerol (Table 1) exhibited a visually liquid appearance and a translucent aspect depending on the polysaccharide used. These observations suggested adequate spreading and distribution of the formulations during film formation.

HPMC formed a homogeneous and translucent gel, a behavior associated with its reversible thermal gelation properties [5]. This characteristic promotes the fluidity and uniform distribution of FFS during the casting process. The system exhibited a decrease in viscosity from η_0 = 2.17 ± 0.02 Pa·s to η_∞ = 0.01 ± 0.00 Pa·s as shear rate increased, which is characteristic of pseudoplastic systems.

Chitosan showed complete solubilization under acidic conditions due to the protonation of its available amino groups. Its moderate degree of deacetylation (75%) indicates that a substantial fraction of the polymer contains free amino groups capable of protonation, favoring polymer chain dispersion and intermolecular interactions [6], and consequently influencing system viscosity. The chitosan-based system exhibited viscosities ranging from η_0 = 0.74 ± 0.26 Pa·s to η_∞ = 0.14 ± 0.01 Pa·s, consistent with more fluid systems showing lower shear-rate dependence.

In contrast, starch showed a noticeable increase in system consistency after gelatinization temperature, associated with the thickening effect of amylopectin (73%) and the structuring and gelling contribution of amylose (27%) [8]. The starch-based formulation displayed viscosities ranging from η_0 = 13.05 ± 2.31 Pa·s to η_∞ = 0.004 ± 0.00 Pa·s, charac-

teristic of systems with high initial viscosity and pronounced shear-thinning behavior as shear rate increased.

3.1.2. Flow Behavior of Film-Forming Solutions

The apparent viscosity of insoluble collagen from *Octopus maya* (CIPM) was 190.36 ± 19.43 Pa·s at 1 s^{-1}. The high viscosity observed may be attributed to the insoluble nature of CIPM and to structural features commonly reported for insoluble collagen systems, including fibrillar organization and viscoelastic network formation, which contribute to increased resistance to flow [25]. Fitting of the experimental curves to the Carreau–Yasuda model ($R^2 > 0.99$) revealed high zero-shear viscosity values (η_0CIPM = 47,944 ± 5318 Pa·s; η_0FFS-CIPM = 5830 ± 1539 Pa·s), followed by a decrease to low infinite-shear viscosity values (η_∞CIPM = 78.15 ± 41.22 Pa·s and η_∞FFS-CIPM = 0.75 ± 0.33 Pa·s). This behavior reflects a progressive reduction in flow resistance as the shear rate increases.

Subsequent homogenization of CIPM in 0.04 M HCl was associated with the partial disruption of intermolecular interactions and improved collagen dispersion within the system [26]. After glycerol incorporation into the homogenized CIPM (Table 1), a homogeneous FFS-CIPM with lower apparent viscosity (33.95 ± 5.69 Pa·s) was obtained, indicating reduced flow resistance compared with the original CIPM and promoting a more fluid behavior (Figure 1). Previous studies on aqueous collagen solutions have demonstrated that viscosity strongly depends on collagen concentration and intermolecular interactions. Kawamata et al. [27] reported a progressive increase in viscosity with increasing tilapia collagen concentration, attributing this behavior to the formation of network-like structures among collagen molecules in aqueous solution. The same authors also observed that HCl addition significantly reduced the system viscosity (from 113 to 68 mPa·s), suggesting a weakening of the interactions responsible for network formation. In this context, the lower viscosity observed for FFS-CIPM may be associated with the collagen concentration used (3%), with the incorporation of 0.04 M HCl and glycerol during formulation, conditions that promote more fluid and processable systems for applications such as film-forming solutions.

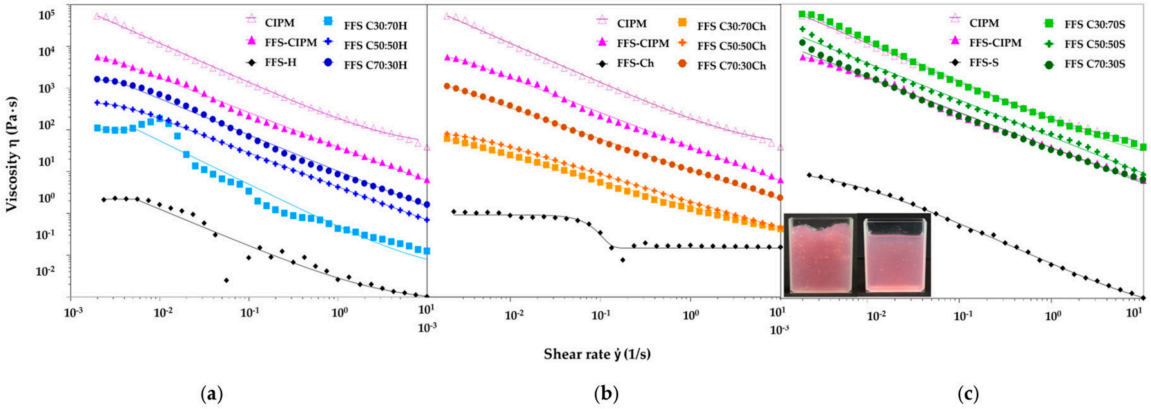


Figure 1. Viscosity (η) curves as a function of shear rate ($\dot{\gamma}$) (10^{-3}–10^{1} s^{-1}) for FFS-CIPM combined with FFS-PS (⧫): (**a**) hydroxypropyl methylcellulose (H), (**b**) chitosan (Ch), and (**c**) starch (S), at FFS-CIPM:FFS-PS ratios of 30:70 (■), 50:50 (✚), and 70:30 (●). Reference curves for insoluble collagen from *Octopus maya* (CIPM, △, left embedded figure) and FFS-CIPM (▲, right embedded figure).

In general, after polysaccharide incorporation into FFS-CIPM, formulations containing HPMC and chitosan maintained viscosities below 11 Pa·s (Table 2) and without significant differences according to the statistical analysis. In both cases, the formulations maintained fluid behavior as the polysaccharide proportion increased, suggesting a limited contribution of these polysaccharides to the rheological response of the system; therefore, they did not promote high flow resistance.

Table 2. Apparent viscosity (η) values measured at 1 s^{-1} and the Carreau-Yasuda model parameters, including zero-shear viscosity (η_0), infinite-shear viscosity (η_∞), consistency index (*k*), flow behavior index (*n*), and transition parameter (α), of the different FFS formulations. Results are expressed as mean ± standard deviation (*n* = 2).

Proportion (%) (FFS-CIPM:FFS-PS)		η (Pa·s)	η_0 (Pa·s)	η_∞ (Pa·s)	*k* (s)	*n*	α
HPMC	100H *	0.02 ± 0.00	2.17 ± 0.02	0.01 ± 0.00	179.30 ± 9.11	0.01 ± 0.14	47.19 ± 52.90
	C30:70H	0.3 ± 0.05 ^{a,B}	35.84 ± 32.51 ^{a,B}	0.03 ± 0.00 ^{a,A}	151.85 ± 58.13 ^{a,A}	0.09 ± 0.13 ^{a,A}	72.28 ± 0.50 ^{a,A}
	C50:50H	3.14 ± 0.38 ^{a,A}	412.49 ± 8.62 ^{a,A}	0.04 ± 0.004 ^{a,A}	445.44 ± 17.60 ^{a,A}	0.21 ± 0.01 ^{a,A}	30.49 ± 33.88 ^{a,A}
	C70:30H	8.43 ± 0.16 ^{a,A}	1454.70 ± 170.03 ^{a,A}	0.10 ± 0.004 ^{a,A}	360.48 ± 44.41 ^{a,B}	0.15 ± 0.03 ^{a,A}	8.41 ± 0.04 ^{a,A}
Chitosan	100Ch *	0.17 ± 0.01	0.74 ± 0.26	0.14 ± 0.01	4.81 ± 5.44	−1342.30 ± 1871.81	5.61 ± 4.05
	C30:70Ch	1.47 ± 0.26 ^{a,B}	109.07 ± 64.69 ^{a,B}	0.06 ± 0.002 ^{a,A}	656.77 ± 200.96 ^{b,A}	0.36 ± 0.04 ^{b,A}	35.76 ± 0.25 ^{a,A}
	C50:50Ch	1.84 ± 0.02 ^{a,A}	110.87 ± 33.28 ^{a,A}	0.04 ± 0.002 ^{a,A}	540.72 ± 274.14 ^{b,A}	0.35 ± 0.003 ^{b,A}	21.70 ± 27.53 ^{a,A}
	C70:30Ch	10.44 ± 0.59 ^{a,A}	1052.64 ± 76.75 ^{a,A}	0.23 ± 0.11 ^{a,A}	481.23 ± 2.04 ^{b,B}	0.25 ± 0.01 ^{b,A}	68.09 ± 3.21 ^{a,A}
Starch	100S *	0.05 ± 0.02	13.05 ± 2.31	0.00 ± 0.00	530.29 ± 448.04	0.07 ± 0.11	11.99 ± 15.83
	C30:70S	197.53 ± 80.21 ^{b,B}	103,631 ± 141,16.68 ^{b,B}	1.37 ± 1.38 ^{a,A}	979.71 ± 336.09 ^{c,A}	0.09 ± 0.03 ^{a,A}	37.93 ± 24.15 ^{a,A}
	C50:50S	79.63 ± 1.61 ^{b,A}	23,410.85 ± 3955.91 ^{b,A}	2.10 ± 2.91 ^{a,A}	808.64 ± 66.03 ^{c,A}	0.09 ± 0.05 ^{a,A}	42.75 ± 10.64 ^{a,A}
	C70:30S	33.54 ± 0.60 ^{b,A}	23,665.80 ± 830.85 ^{b,A}	0.06 ± 0.06 ^{a,A}	1864.20 ± 86.75 ^{c,B}	0.14 ± 0.01 ^{a,A}	13.33 ± 0.98 ^{a,A}

PS: Polysaccharide; FFS: Film-forming solution. CIPM or C: Insoluble collagen from *Octopus maya*; HPMC or H: Hydroxypropyl methylcellulose; Ch: Chitosan; S: Starch. Different letters correspond to significant differences within a column by: (a) type of polysaccharide (lower case), (b) proportion (upper case). Controls were not included in the ANOVA. * Some fitting parameters of the model in the control formulations (fluid behavior) exhibited high standard deviations, indicating limited estimation of the model coefficients.

HPMC-based systems showed a progressive decrease in viscosity as the HPMC fraction increased (Figure 1a). Apparent viscosity increased with CIPM content in FFS-H, ranging from 0.024 ± 0.003 Pa·s for the individual FFS-H system to 8.43 ± 0.16 Pa·s for C70:30H (Figure 1a). A similar trend was reported by Ding et al. [28] in systems formulated with type I collagen extracted from calf skin and HPMC. In collagen:HPMC mixtures (70:30, 50:50, and 30:70), viscosities of approximately 90, 60, and 30 Pa·s, respectively, were observed as the polysaccharide fraction increased, compared with 120 Pa·s for collagen alone at a shear rate of ~1 s^{-1}. Although the viscosities reported by these authors were higher than those obtained in the present study, likely due to differences in collagen origin and composition, both studies agree that increasing HPMC content promotes more fluid systems with lower flow resistance. This behavior has previously been associated with reduced structural organization within the protein network [28,29]. Therefore, formulations with higher HPMC content may have potential applications in systems requiring high fluidity and easy spreading, such as spray-applied coatings and film-forming solutions.

In chitosan-based systems, viscosity increased as the proportion of CIPM increased (ηC70:30Ch > ηC50:50Ch > ηC30:70Ch) (Figure 1b), reaching values between 1.47 ± 0.26 and 10.44 ± 0.59 Pa·s (Table 2). The rheological behavior observed at higher collagen proportions may be associated with the greater contribution of CIPM to the overall viscosity of the system, whereas the contribution of chitosan remained limited by its moderate degree of deacetylation (DA = 75%), which partially restricts its interaction capacity under acidic conditions. As a result, CIPM acted as the main component responsible for the increase in flow resistance as its proportion increased. Similarly, Heidenreich et al. [30] reported that collagen–chitosan mixtures maintain higher viscosities only when collagen acts as the predominant structural component, favoring the formation of denser and more stable matrices. Accordingly, C30:70Ch and C50:50Ch, which contained lower collagen proportions, exhibited relatively low viscosities (1.47 ± 0.26 and 1.84 ± 0.02 Pa·s, respectively). The observed trend is also consistent with the findings of Zheng et al. [31], who evaluated type I collagen extracted from calf skin combined with chitosan of a higher deacetylation degree (95%) than that used in the present study (75%). These authors reported a significant decrease in viscosity as the chitosan proportion increased, from 862.54 to 0.60 Pa·s at 0.05 s^{-1}. Together, these results suggest that increasing chitosan content promotes more fluid systems with lower flow resistance, regardless of collagen source.

Overall, viscosity increased with increasing collagen proportion in all systems except those formulated with starch, in which the highest viscosities were observed as the starch fraction increased (Figure 1c). In contrast to the behavior of the other polysaccharides, decreasing the FFS-CIPM fraction while increasing FFS-S significantly increased viscosity (up to 197.53 ± 80.21 Pa·s; Table 2). This behavior may be attributed to the ability of starch granules to swell as the temperature increases and interact with the protein matrix, forming denser networks with greater resistance to flow at low shear rates. Such protein–starch associations have been described as an interaction capable of modifying texture and increasing gel viscosity in food systems [8]. These results suggest that although starch alone exhibited low viscosity (0.049 ± 0.02 Pa·s), its combination with collagen resulted in a marked increase in viscosity, reflecting an interaction effect between both biopolymers on the rheological response of the system (Figure 1c).

In addition to the differences in apparent viscosity among formulations, the flow curves revealed important changes in the rheological response of the systems as the shear rate increased. CIPM, FFS-CIPM, and the polysaccharide-containing formulations all exhibited pronounced pseudoplastic behavior (Figure 1). This behavior was confirmed by fitting the data to the Carreau-Yasuda model, in which all systems showed flow behavior index (n) values lower than 1, characteristic of pseudoplastic fluids [32]. On the other

hand, starch-based formulations exhibited the highest zero-shear viscosity (η_0) values, particularly C30:70S and C50:50S, whereas systems formulated with HPMC and chitosan showed considerably lower values. These results indicate greater initial flow resistance in the presence of starch and more fluid behavior in HPMC and chitosan-based formulations.

The FFS-CIPM:FFS-PS formulations (30:70, 50:50, and 70:30) allowed evaluation of the effects of polysaccharide type (A) and collagen-to-polysaccharide ratio (B) on formulation viscosity. Statistical analysis showed that both factors, as well as their interaction (A × B), significantly affected system viscosity ($p < 0.05$) (Table 3). These findings indicate that the effect of CIPM on flow behavior depended on the polysaccharide used, resulting in distinct rheological responses among formulations, particularly in starch-based systems, where increasing the polysaccharide proportion caused a marked increase in viscosity (Figure 2a).

Table 3. Effects of studied factors: polysaccharide type, proportion, and their interaction on flow behavior based on the Carreau-Yasuda model parameters (*p*-values).

Factors	η_0 (Pa·s)	η_∞ (Pa·s)	k (s)	n	α
Polysaccharide type (A)	<0.0001	0.1835	<0.0001	0.0001	0.5833
Proportion (B)	<0.0001	0.6441	0.0159	0.4592	0.1653
A × B	<0.0001	0.6087	0.0028	0.1101	0.0177

η_0 corresponds to the zero-shear viscosity (low shear-rate viscosity), η_∞ to the infinite-shear viscosity (high shear-rate viscosity), k to the consistency index, n to the flow behavior index, and α to the transition parameter.

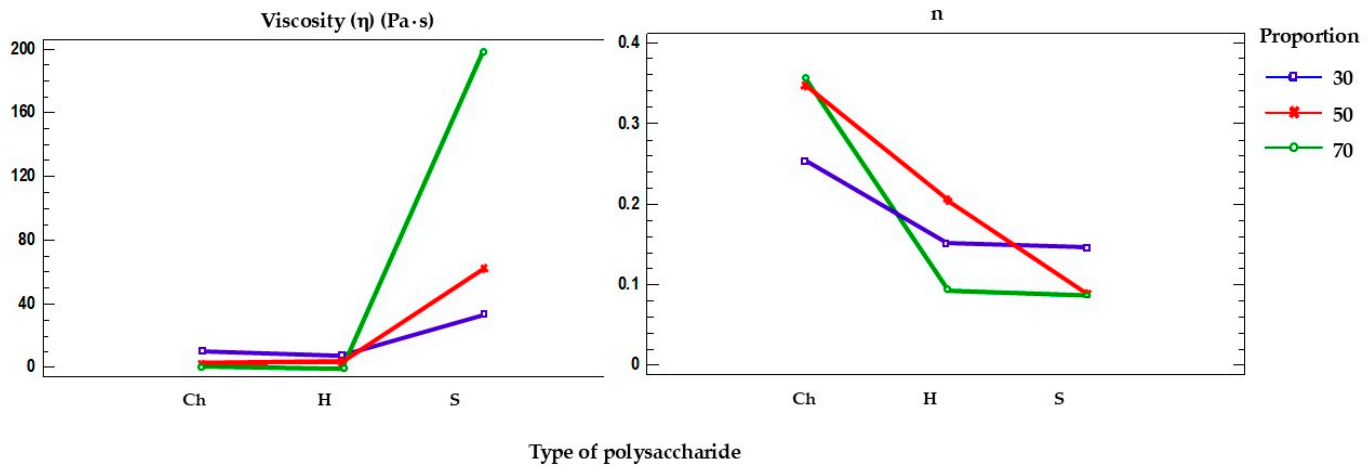


Figure 2. Interaction plots between polysaccharide type and the FFS-CIPM:FFS-PS ratio on the Carreau–Yasuda model parameters: (**a**) apparent viscosity (η) and (**b**) flow behavior index (n). Lines represent the 30:70, 50:50, and 70:30 ratios. H: Hydroxypropyl methylcellulose; Ch: Chitosan; S: Starch.

Multifactorial analysis revealed that polysaccharide type (A), the FFS-CIPM:FFS-PS ratio (B), and their interaction (A × B) significantly affected ($p < 0.05$) several parameters of the Carreau-Yasuda model. The η_0 parameter showed significant effects for all evaluated factors, indicating that formulation composition modified the initial viscosity of the system under low shear-rate conditions, which reflects differences in the rheological contribution of collagen and polysaccharides under low shear-rate conditions. In contrast, η∞ showed no significant differences ($p > 0.05$) for any of the evaluated factors, suggesting that at high shear rates the formulations tended toward similar flow behavior. The k parameter was also significantly influenced by polysaccharide type, proportion, and their interaction, indicating that formulation composition affected the viscosity, decreasing as the shear rate

increased. The flow behavior index (n) was affected only by polysaccharide type, suggesting that the chemical nature influenced the degree of pseudoplasticity of the formulations. As shown in Figure 2b, formulations containing chitosan exhibited the highest n values, whereas those formulated with HPMC and starch showed lower values. Although slight variations in n were observed among formulations, the interaction between polysaccharide type and proportion was not significant ($p > 0.05$), indicating that the effect of proportion on this parameter was similar across all systems. Therefore, pseudoplastic behavior depended mainly on the polysaccharide employed rather than on the specific combination of both factors. Likewise, the transition parameter α showed a significant effect only for the A × B interaction, indicating that the transition between the Newtonian region and pseudoplastic behavior depended on the specific combination of polysaccharide type and formulation ratio. Finally, apparent viscosity (η) was significantly affected by all evaluated factors, demonstrating that formulation composition modified both the magnitude of viscosity and its response to increasing shear rate.

3.2. Viscoelastic Behavior of Systems

Frequency sweep tests of CIPM and FFS-CIPM (Figure 3) showed that, in both systems, the storage modulus (G′) remained higher than the loss modulus (G″), with tan δ values lower than 1. Both G′ and G″ increased with frequency in all formulations; however, this increase was more pronounced in the polysaccharide control systems, whereas CIPM and several FFS-CIPM:FFS-PS formulations exhibited a weaker frequency dependence. Such behavior may be associated with the presence of more organized viscoelastic structures within the system. Overall, these results confirm the typical viscoelastic response of gel systems, in which the elastic component of the network predominates [3]. CIPM exhibited a markedly elastic behavior, with G′ (1.51 ± 0.03 Pa) exceeding G″ (0.19 ± 0.01 Pa) and a low tan δ value (0.13 ± 0.005), suggesting a relatively organized viscoelastic structure. This pattern is similar to that reported for collagen gels composed of densely packed fibrillar networks, characterized by minimal dissipation of the energy stored within the structure [25].

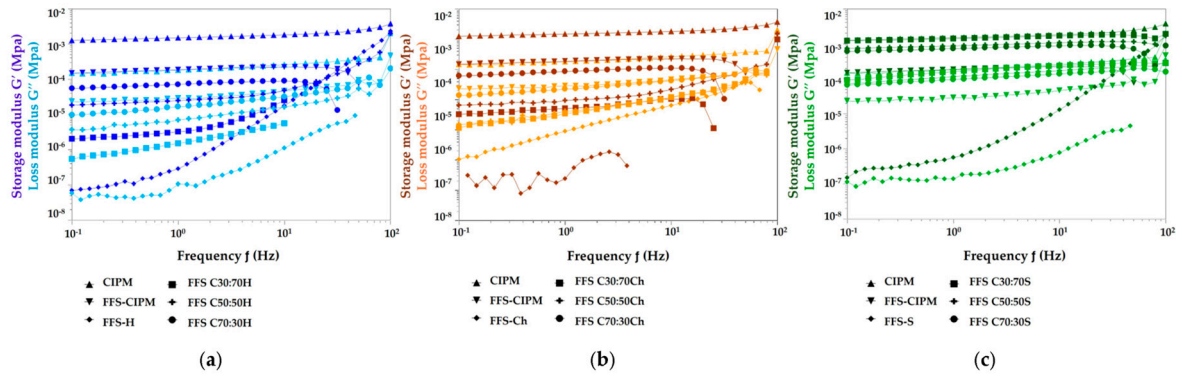


Figure 3. Viscoelastic curves showing storage modulus (G′) and loss modulus (G″) as a function of frequency (f) (10^{-1}–10^{2} Hz) for polysaccharides (PS, ♦): (**a**) hydroxypropyl methylcellulose (H), (**b**) chitosan (Ch), and (**c**) starch (S), at FFS-CIPM:FFS-PS ratios of 30:70 (■), 50:50 (✚), and 70:30 (●). Reference curves for insoluble collagen from *Octopus maya* (CIPM, ▲) and FFS-CIPM (▼).

In contrast, FFS-CIPM exhibited significantly lower moduli (G′ = 0.18 ± 0.01 Pa; G″ = 0.03 ± 0.002 Pa), indicating a lower elastic response and a more fluid viscoelastic behavior. This reduction may be associated with structural changes occurring during acid solubilization and with the plasticizing effect of glycerol. According to Ghani et al. [25], less compact systems tend to exhibit higher G″ and tan δ values because of the greater mobility of polymer chains. In this context, the more fluid behavior of FFS-CIPM may suggest a

lower degree of structural organization within the system suitable for its function as a film-forming solution. Although G′ remained higher than G″ throughout the entire frequency range, the proximity between both moduli at high frequencies (>50 Hz) may indicate a transition toward liquid-like viscoelastic behavior under more intense or prolonged deformation conditions [32]. A similar behavior was also observed in the FFS-CIPM:FFS-PS systems at 50:50 and 70:30 ratios, regardless of the polysaccharide employed, suggesting that this response was mainly associated with the contribution of collagen within the system (Figure 3).

HPMC-based formulations (Figure 3a) exhibited the lowest G′ and G″ values (Table 4), particularly when the polysaccharide predominated in the system. The reduction in viscoelastic moduli suggests that the structural network formed between collagen and HPMC had a limited elastic contribution and a reduced capacity to store energy during oscillatory deformation, a behavior also reported by Ding et al. [28] in systems containing high HPMC concentrations. This weak structuring may be explained by the predominantly physical interactions established between both biopolymers [33], which limit the formation of strong three-dimensional networks. In addition, the presence of glycerol in the FFS further reduced network rigidity, thereby weakening the already limited interactions between collagen and HPMC and explaining the low G′ values observed in systems with higher HPMC content. Nevertheless, this behavior may represent a technological advantage, since systems with lower viscoelastic resistance favor the spreading and leveling of film-forming solutions during the drying process.

Table 4. Storage modulus (G′), loss modulus (G″), and tan δ values of film-forming solutions (FFS). Results are expressed as mean ± standard deviation (n = 2).

Proportion (%) (FFS-CIPM:FFS-PS)		G′ (Storage Modulus) (Pa)	G″ (Loss Modulus) (Pa)	tan δ (Tangent Delta)
HPMC	C30:70H	0.004 ± 0.001 ^{a,B}	0.002 ± 0.0003 ^{a,B}	0.44 ± 0.05 ^{b,B}
	C50:50H	0.020 ± 0.001 ^{a,A}	0.007 ± 0.0000 ^{a,A}	0.29 ± 0.01 ^{b,B}
	C70:30H	0.070 ± 0.001 ^{a,A}	0.017 ± 0.0007 ^{a,A}	0.23 ± 0.01 ^{b,A}
Chitosan	C30:70Ch	0.006 ± 0.002 ^{a,B}	0.003 ± 0.0002 ^{a,B}	0.54 ± 0.18 ^{c,B}
	C50:50Ch	0.008 ± 0.002 ^{a,A}	0.004 ± 0.0005 ^{a,A}	0.47 ± 0.05 ^{c,B}
	C70:30Ch	0.089 ± 0.004 ^{a,A}	0.023 ± 0.0000 ^{a,A}	0.26 ± 0.01 ^{c,A}
Starch	C30:70S	1.35 ± 0.057 ^{b,B}	0.155 ± 0.0071 ^{b,B}	0.12 ± 0.00 ^{a,B}
	C50:50S	0.880 ± 0.023 ^{b,A}	0.118 ± 0.0007 ^{b,A}	0.14 ± 0.01 ^{a,B}
	C70:30S	0.750 ± 0.046 ^{b,A}	0.098 ± 0.0028 ^{b,A}	0.13 ± 0.00 ^{a,A}

Different letters correspond to significant differences within a column by: (a) type of polysaccharide (lower case), (b) proportion (upper case).

Likewise, in chitosan-based formulations (Figure 3b), increasing collagen content strengthened the viscoelastic response of the system. The C70:30Ch formulation exhibited the highest G′ and G″ values (Table 4) and the lowest tan δ value (0.26 ± 0.01), indicating a predominantly elastic behavior (G′ > G″) at frequencies below 50 Hz. However, at higher frequencies, a crossover between both moduli was observed, suggesting that the system tended to dissipate energy to a greater extent than to store it elastically. From an application perspective, this behavior could favor the fluidity and leveling of the FFS during film formation. Nevertheless, the lower viscoelastic stability at high frequencies may affect the structural uniformity of the system prior to drying, potentially compromising the final mechanical resistance of the film.

As chitosan content increased, both viscoelastic moduli decreased while tan δ increased, reflecting a gradual loss of structural organization. In C30:70Ch (tan δ = 0.54 ± 0.18), lower modulus values were observed (Table 4), together with a reduced initial separation between G′

and G″ (Figure 3b), indicating a weaker network that progressively lost its elastic dominance at high frequencies. Although all formulations exhibited tan δ values lower than 1, confirming the predominance of elastic behavior, the increase in tan δ with higher chitosan content indicates a shift toward more viscous behavior, which may favor extensibility properties in coating applications. This trend is consistent with the findings of Zheng et al. [31], who reported that high chitosan contents reduced viscoelastic moduli and increased tan δ values (>1), reflecting weakening of the collagen-chitosan network. However, glycerol reduced the rigidity of all systems; therefore, even though C30:70Ch exhibited more viscous behavior at high frequencies, tan δ values did not exceed 1.

All starch-based systems maintained low tan δ values (0.12–0.14) and a pronounced elastic dominance (G′ > G″), indicating a stable viscoelastic network throughout the frequency sweep. Although a slight decrease in G′ was observed at high frequencies, the elastic behavior of the system remained predominant (Figure 3c). Unlike the HPMC and chitosan-based systems, in which increasing polysaccharide proportion reduced the viscoelastic moduli and promoted more fluid systems, starch-based formulations exhibited the opposite behavior. Increasing starch content enhanced the viscoelastic moduli, particularly in the C30:70S system (G′ = 1.35 ± 0.057 Pa), demonstrating a greater capacity to store elastic energy. This behavior is consistent with the protein-starch associations described in the literature, where starch granule swelling and physicochemical interactions promote the formation of more rigid and cohesive networks [8]. Overall, these results suggest that starch acts as a structuring agent in collagen-based systems.

Overall, the results demonstrate that the viscoelastic behavior of the systems depended primarily on polysaccharide type and, to a lesser extent, on the formulation ratio, reflecting differences associated with the chemical nature and compatibility of the biopolymers. Consistent with these observations, statistical analysis showed that both G′ and G″ were significantly affected by polysaccharide type, proportion, and their interaction ($p < 0.05$), indicating that the effect of formulation ratio depended on the polysaccharide employed (Table 5; Figure 4a). In contrast, tan δ showed no significant interaction effect ($p > 0.05$), indicating that the balance between elastic and viscous components responded similarly to changes in formulation ratio regardless of the polysaccharide used (Table 5; Figure 4b). These findings demonstrate that both polysaccharide selection and formulation ratio can be used to modulate the rheological and viscoelastic properties of FFS-CIPM:FFS-PS systems. This allows the differentiation of systems with lower elastic response and greater deformability, potentially suitable for coatings requiring good extensibility, from more elastic and structured systems that may favor the formation of films with higher mechanical integrity. Overall, these results highlight the potential of collagen-polysaccharide systems for designing matrices with tunable properties according to their intended application as biodegradable films.

Table 5. Effects of the studied factors, polysaccharide type, proportion, and their interaction, on G′ (storage modulus), G″ (loss modulus), and tan δ values, which describe the balance between the elastic and viscous components of the system.

	Table of *p*-Values		
	G′ (Pa)	**G″ (Pa)**	**tan δ**
Polysaccharide type (A)	<0.0001	<0.0001	0.0001
Proportion (B)	<0.0001	0.0002	0.0069
A × B	<0.0001	<0.0001	0.0703

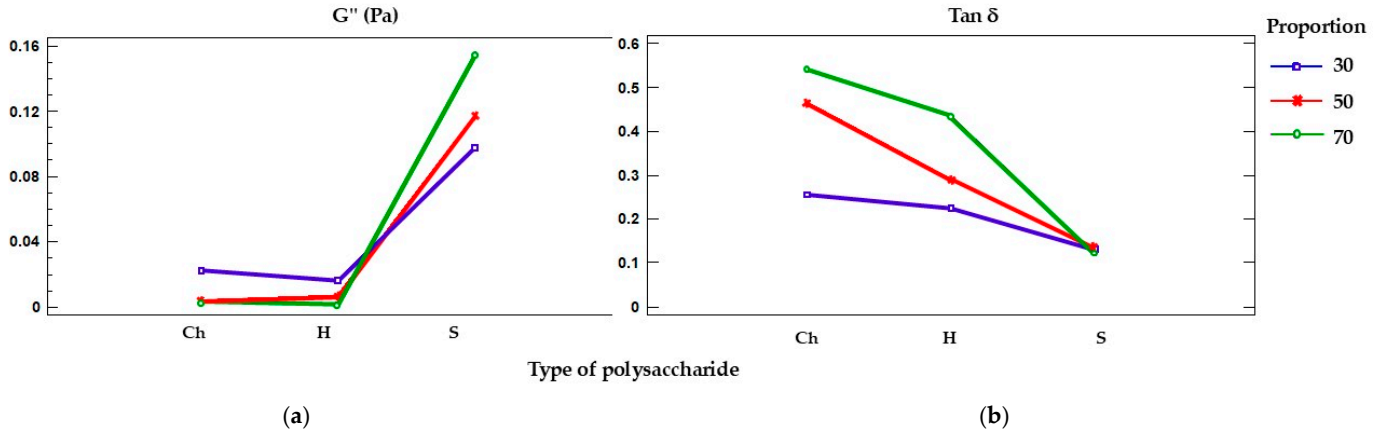


Figure 4. Effect of the interaction between polysaccharide type and the FFS-CIPM:FFS-PS ratio on the viscoelastic behavior of the formulations: (**a**) storage modulus (G″) and (**b**) tan δ. Lines represent the 30:70, 50:50, and 70:30 ratios. H: Hydroxypropyl methylcellulose, Ch: Chitosan, S: Starch.

4. Conclusions

The valorization of *Octopus maya* by-products enabled the extraction of insoluble collagen (CIPM) with suitable functionality for incorporation into film-forming solutions (FFS) combined with food-grade polysaccharides. The rheological properties of the systems could be modulated through the selection of polysaccharide type and proportion, directly influencing both flow behavior and viscoelastic response. Starch-based FFS formed denser and more rigid matrices, suggesting their potential suitability for applications requiring high flow resistance, such as thick coatings or gels that must maintain structural integrity during drying. In contrast, formulations containing HPMC and chitosan produced more fluid systems, suggesting their potential suitability for spray-applied coatings, atomization processes, or FFS that require rapid spreading over surfaces. These potential applications are inferred from the rheological properties of the formulations and were not experimentally validated in the present study. In addition, all formulations exhibited pseudoplastic behavior, with flow behavior index values lower than 1 ($n < 1$), a favorable characteristic for achieving uniform spreading on surfaces. Overall, these findings confirm the potential of collagen from *Octopus maya* as a versatile functional ingredient for the development of biomaterials, coatings, and film-forming solutions with tunable rheological properties tailored to specific technological applications, while simultaneously contributing to the sustainable utilization of local marine resources.

Supplementary Materials: The following supporting information can be downloaded at: https://www.mdpi.com/article/10.3390/pr14132205/s1, Figure S1: Samples: (1) Thermo Scientific molecular weight marker; (2) bovine type I collagen standard (100 µg in 10 µL of 0.02 M HCl mixed with 50 µL Laemmli sample buffer); (3) CIPM resuspended in 200 µL of 1% SDS (100 µL of suspension mixed with 100 µL Laemmli sample buffer); and (4) CIPM mixed with 50 µL Laemmli sample buffer; Table S1: Quantification of total amino acids in the insoluble collagen fraction (CIPM) from *Octopus maya* by-products using UPLC-QDa.

Author Contributions: Conceptualization, M.O.R.-S., I.M.R.-B., É.G.-M. and M.F.A.-P.; methodology, M.O.R.-S., I.M.R.-B., J.V.C.-R., É.G.-M. and M.F.A.-P.; software, M.O.R.-S., I.M.R.-B., É.G.-M. and M.F.A.-P.; validation, M.O.R.-S., I.M.R.-B. and J.V.C.-R.; formal analysis, M.O.R.-S., I.M.R.-B., É.G.-M. and M.F.A.-P.; investigation, M.O.R.-S. and M.F.A.-P.; resources, M.O.R.-S.; data curation, M.O.R.-S.; writing—original draft preparation, M.F.A.-P.; writing—review and editing, M.O.R.-S., I.M.R.-B., É.G.-M. and M.F.A.-P.; visualization, I.M.R.-B.; supervision, M.O.R.-S.; project administration, M.O.R.-S.; funding acquisition, M.O.R.-S. All authors have read and agreed to the published version of the manuscript.

Funding: To the Project 6559 "Plataforma Tecnológica Pulpo maya para el Desarrollo de Productos de Alto Valor Agregado" and to SECIHTI for the scholarship No. 4000427 granted to author María Fernanda Acosta-Pacheco.

Data Availability Statement: The original contributions presented in this study are included in the article/Supplementary Materials. Further inquiries can be directed to the corresponding author.

Acknowledgments: To the SELTA Food Lab of the Southeast Headquarters of the CIATEJ for the support and technical assistance in Rheological data acquisition and analysis.

Conflicts of Interest: The authors declare no conflicts of interest.

References

1. Zhao, Y.; Li, B.; Li, C.; Xu, Y.; Luo, Y.; Liang, D.; Huang, C. Comprehensive review of polysaccharide-based materials in edible packaging: A sustainable approach. *Foods* **2021**, *10*, 1845. [CrossRef] [PubMed]
2. Guo, Y.; Ma, C.; Xu, Y.; Du, L.; Yang, X. Food gels based on polysaccharide and protein: Preparation, formation mechanisms, and delivery of bioactive substances. *Gels* **2024**, *10*, 735. [CrossRef] [PubMed]
3. Saha, D.; Bhattacharya, S. Hydrocolloids as thickening and gelling agents in food: A critical review. *J. Food Sci. Technol.* **2010**, *47*, 587–597. [CrossRef] [PubMed]
4. Nieto, M.B. Structure and function of polysaccharide gum-based edible films and coatings. In *Edible Films and Coatings for Food Applications*; Huber, K., Embuscado, M., Eds.; Springer: Berlin/Heidelberg, Germany, 2009; pp. 57–112. [CrossRef]
5. Zhang, H.; Zhang, F.; Yuan, R. Applications of natural polymer-based hydrogels in the food industry. In *Hydrogels Based on Natural Polymers*; Reddy, E.M.M., Mishra, A.K., Thakur, M., Eds.; Elsevier: Amsterdam, The Netherlands, 2020; pp. 357–410. [CrossRef]
6. Aranaz, I.; Alcántara, A.R.; Civera, M.C.; Arias, C.; Elorza, B.; Heras Caballero, A.; Acosta, N. Chitosan: An overview of its properties and applications. *Polymers* **2021**, *13*, 3256. [CrossRef] [PubMed]
7. Mitantsoa, J.T.; Ravelonandro, P.H.; Andrianony, F.A.; Andrianaivoravelona, R.R. Elaboration and characterization of bioplastic films based on bitter cassava starch (Manihot esculenta) reinforced by chitosan extracted from crab (*Shylla seratta*) shells. *arXiv* **2023**, arXiv:2310.15172. [CrossRef]
8. Zhang, Y.; Li, S.; Yu, J.; Wang, S. The effect of protein–starch interaction on the structure and properties of starch and its application in flour products. *Foods* **2025**, *14*, 778. [CrossRef]
9. Meisenberg, G.; Simmons, W.H. *Principios de Bioquímica Médica*, 4th ed.; Elsevier: Amsterdam, The Netherlands, 2018.
10. Ahmad, M.I.; Li, Y.; Pan, J.; Liu, F.; Dai, H.; Fu, Y.; Huang, T.; Farooq, S.; Zhang, H. Collagen and gelatin: Structure, properties, and applications in food industry. *Int. J. Biol. Macromol.* **2024**, *254*, 128037. [CrossRef] [PubMed]
11. Ricard-Blum, S. The collagen family. *Cold Spring Harb. Perspect. Biol.* **2011**, *3*, a004978. [CrossRef] [PubMed]
12. Ahmed, M.; Verma, A.K.; Patel, R. Collagen extraction and recent biological activities of collagen peptides derived from sea-food waste: A review. *Sustain. Chem. Pharm.* **2020**, *18*, 100315. [CrossRef]
13. Farooq, S.; Ahmad, M.I.; Zheng, S.; Ali, U.; Li, Y.; Shixiu, C.; Zhang, H. A review on marine collagen: Sources, extraction methods, colloids properties, and food applications. *Collagen Leather* **2024**, *6*, 11. [CrossRef]
14. Comisión Nacional de Acuacultura y Pesca. Anuario Estadístico de Acuacultura y Pesca 2023. Secretaría de Agricultura y Desarrollo Rural. 2023. Available online: https://nube.conapesca.gob.mx/sites/cona/dgppe/2023/ANUARIO_ESTADISTICO_DE_ACUACULTURA_Y_PESCA_2023.pdf (accessed on 15 January 2026).
15. Ocampo-García, L. Extracción de Colágeno de Subproductos de Pulpo maya (*Octopus maya*) y su Caracterización Tecnofuncional. Master's Thesis, Centro de Investigación y Asistencia en Tecnología y Diseño del Estado de Jalisco, A.C., Guadalajara, Mexico, 2022.
16. Tapia Vásquez, A.E. Identificación y Caracterización Estructural de los Diferentes Tipos de Piridinolina Presentes en Fibras de Colágeno de Pulpo (*Octopus vulgaris*) y Calamar Gigante (*Dosidicus gigas*). Ph.D. Thesis, Universidad de Sonora, Hermosillo, Mexico, 2022.
17. Torres-Arreola, W.; Pacheco-Aguilar, R.; Sotelo-Mundo, R.; Rouzaud-Sandez, O.; Ezquerra-Brauer, J.Y. Caracterización parcial del colágeno extraído a partir del manto, aleta y tentáculos de calamar gigante (*Dosidicus gigas*). *Cienc. Tecnol. Aliment.* **2008**, *6*, 101–108. [CrossRef]
18. Moscoso, J.L.A. Estudio de Biopelículas de Compósitos de Colágeno de Calamar Gigante (*Dosidicus gigas*) y Quitosina. Master's Thesis, Universidad de Sonora, Hermosillo, Mexico, 2009.
19. Sánchez-Soto, J.M.; López-Alcántara, R.; Sánchez-González Adel, P.; Torres-Mendoza, E.J. Evaluation of mechanical properties of matrices derived from fish scale collagen. *Rev. Colomb. Investig. Agroindustriales* **2022**, *9*, 119–129. [CrossRef]
20. Ulfariati, C.; Aprilia, S.; Munawar, A.A. Development of biocomposite edible film food packaging based on gelatin from chicken claw waste. *Case Stud. Chem. Environ. Eng.* **2023**, *8*, 100371. [CrossRef]

21. Ribeiro, A.M.; Estevinho, B.N.; Rocha, F. Preparation and incorporation of functional ingredients in edible films and coatings. *Food Bioprocess Technol.* **2021**, *14*, 209–231. [CrossRef]
22. Chakravartula, S.S.N.; Soccio, M.; Lotti, N.; Balestra, F.; Dalla Rosa, M.; Siracusa, V. Characterization of composite edible films based on pectin/alginate/whey protein concentrate. *Materials* **2019**, *12*, 2454. [CrossRef]
23. Rossman, J.M. Commercial manufacture of edible films. In *Edible Films and Coatings for Food Applications*; Huber, E.K., Embuscado, M., Eds.; Springer: Berlin/Heidelberg, Germany, 2009; pp. 367–390. [CrossRef]
24. Ramírez-Sucre, M.O.; Baigts-Allende, D.K. Efecto del tratamiento térmico en el comportamiento reológico de salsas de chile habanero (*Capsicum chinense*) adicionadas con gomas guar y xantana. *Agrociencia* **2016**, *50*, 837–847. Available online: http://www.scielo.org.mx/scielo.php?script=sci_arttext&pid=S1405-31952016000700837 (accessed on 28 November 2025).
25. Ghani, A.; Okada, M.; Sun, B.; Zhang, X.; Higuchi, I.; Takagi, Y. Comparative Study of the Gel-Forming Ability of Type I Collagens Extracted from Different Organs and Fish Species. *Gels* **2025**, *11*, 533. [CrossRef] [PubMed]
26. Gonapinuwala, S.T.; Kirk, S.; Jones, J.R.; De Croos, M.D.S.T.; Bronlund, J.E. Collagen with native triple-helical structure from representative cold-water and warm-water fish skins using a modified protocol. *Food Bioprocess Technol.* **2025**, *18*, 7993–8007. [CrossRef]
27. Kawamata, H.; Kuwaki, S.; Mishina, T.; Ikoma, T.; Tanaka, J.; Nozaki, R. Hierarchical viscosity of aqueous solution of tilapia scale collagen investigated via dielectric spectroscopy between 500 MHz and 2.5 THz. *Sci. Rep.* **2017**, *7*, 45398. [CrossRef] [PubMed]
28. Ding, C.; Zhang, M.; Li, G. Rheological properties of collagen/hydroxypropyl methylcellulose (COL/HPMC) blended solutions. *J. Appl. Polym. Sci.* **2014**, *131*, 40042. [CrossRef]
29. Tang, P.; Li, X.; Li, H.; Li, J.; Tang, B.; Zheng, T. Development of active film based on collagen and hydroxypropyl methylcellulose incorporating apple polyphenol for food packaging. *Int. J. Biol. Macromol.* **2024**, *273*, 132960. [CrossRef] [PubMed]
30. Heidenreich, A.C.; Pérez-Recalde, M.; González Wusener, A.; Hermida, É.B. Collagen and chitosan blends for 3D bioprinting: A rheological and printability approach. *Polym. Test.* **2020**, *82*, 106297. [CrossRef]
31. Zheng, T.; Tang, P.; Shen, L.; Bu, H.; Li, G. Rheological behavior of collagen/chitosan blended solutions. *J. Appl. Polym. Sci.* **2021**, *138*, e50840. [CrossRef]
32. Herrada-Manchón, H.; Fernández, M.A.; Aguilar, E. Essential guide to hydrogel rheology in extrusion 3D printing: How to measure it and why it matters? *Gels* **2023**, *9*, 517. [CrossRef] [PubMed]
33. Tang, C.; Zhang, L.; Huang, Q. Mechanisms of gel formation in collagen/hydroxypropyl methylcellulose aqueous mixtures. *Int. J. Biol. Macromol.* **2025**, *251*, 142407. [CrossRef] [PubMed]

Disclaimer/Publisher's Note: The statements, opinions and data contained in all publications are solely those of the individual author(s) and contributor(s) and not of MDPI and/or the editor(s). MDPI and/or the editor(s) disclaim responsibility for any injury to people or property resulting from any ideas, methods, instructions or products referred to in the content.